Available online at www.sciencedirect.com
ScienceDirect
Composites Science and Technology 67 (2007) 2061–2070
COMPOSITES SCIENCE AND TECHNOLOGY
www.elsevier.com/locate/compscitech

The effect of temperature and strain rate on the mechanical properties of highly oriented polypropylene tapes and all-polypropylene composites

B. Alcock [a,*], N.O. Cabrera [a,b], N.-M. Barkoula [a], C.T. Reynolds [a], L.E. Govaert [c], T. Peijs [a,b]

[a] Department of Materials, Queen Mary, University of London, Mile End Road, London E1 4NS, UK
[b] Eindhoven Polymer Laboratories, Eindhoven University of Technology, P.O. Box 513, 5600MB Eindhoven, Netherlands
[c] Materials Technology, Dutch Polymer Institute, Eindhoven University of Technology, P.O. Box 513, 5600 MB Eindhoven, Netherlands

Received 2 August 2006; received in revised form 20 November 2006; accepted 25 November 2006
Available online 23 January 2007

Abstract

The creation of highly oriented, co-extruded polypropylene (PP) tapes allows the production of recyclable "all-polypropylene" (all-PP) composites, with a large temperature processing window and a high volume fraction of highly oriented PP (>90%). The wholly thermoplastic nature of these 'self-reinforced' composites implies that the mechanical performance may vary with temperature. This paper describes the mechanical performance of all-PP composites by measuring the mechanical properties of highly oriented PP tapes and subsequent all-PP composites at a range of temperatures by static and dynamic testing methods. The time–temperature equivalence of all-PP composites is investigated by creating mastercurves of dynamic modulus and tensile strength. A comparison of the performance of these composites with commercial glass fibre reinforced polypropylene composites is included.

Keywords: A. Polymers; A. Recycling; B. High-temperature properties; B. Thermomechanical properties; D. Life prediction

1. Introduction

In a series of recent papers [1–4], composite materials in which both the fibre and the matrix are based on polypropylene (PP) have been described. These so-called "all-PP" composites are designed to compete with traditional thermoplastic composites such as glass fibre reinforced PP, so must possess comparable or superior mechanical properties. One of the main advantages of all-PP composites is the enhanced recyclability which is achieved by using the same polymer for both fibre and matrix phase of the composite. Unlike glass fibre reinforced PP composites, all-PP composites can be entirely melted down at the end of the product life for recycling into PP feedstock. However, the entirely thermoplastic nature of these composites raises important questions regarding the mechanical performance at elevated temperatures and low strain rates.

The concept of improving the mechanical properties of polymers by molecular orientation, without the addition of foreign reinforcements is not new. So-called "self-reinforced polymers" have been the subject of numerous publications focussing on a range of polymers and processing routes including polypropylene [5–8], polyethylene [9–14], polyethylene terephthalate [15–17], polyethylene naphthalate [18], poly(methyl methacrylate) [19–22], polyamide [23] and liquid crystal polymers [24,25]. Numerous studies have also been presented specifically for biomedical applications, where the self-reinforcement of bioresorbable polymers is required for load bearing orthopaedic applications, in which foreign reinforcements may complicate biocompatibility or bioresorption profiles [26,27].

* Corresponding author.
E-mail address: b.alcock@gmail.com (B. Alcock).

0266-3538/$ - see front matter © 2006 Elsevier Ltd. All rights reserved.
doi:10.1016/j.compscitech.2006.11.012

Like many of the ''self-reinforced'' polymers described in literature, the all-PP composites presented in this paper are wholly thermoplastic, and they can be expected to show varying mechanical properties with temperature and strain rate. This can limit the application of such materials and so must be understood. In the general case of partially or wholly amorphous polymers, the effect of temperature and time during mechanical loading can be considered equivalent. For example, loading such a polymer at a high strain rate can be considered equivalent to loading at a low temperature and vice versa. With increasing temperature, the modulus of polymers generally decreases, although thermal transitions occur which can impart a dramatic step-change in stiffness over a relatively small range of temperatures. These thermal transitions are caused by conformational changes becoming possible due to increased thermal energy in the system and can greatly affect the practical applications of a polymer under load. Polypropylene is semi-crystalline and exhibits a complex combination of thermal transitions occurring in the crystalline phase as well as in the amorphous phase. The presence of the crystalline phase can also impose restrictions on the mobility of the amorphous phase, which further complicates the prediction of the mechanical performance of such semi-crystalline polymers at elevated or reduced temperatures.

This paper has two aims. The first aim of this paper is to investigate the response of highly oriented polypropylene tapes to dynamic mechanical loading at a range of temperatures. These highly oriented polypropylene tapes are thermally bonded together to form all-PP composite structures, and so the precursor tapes are solely responsible for the mechanical performance of the resulting composites. The second aim of this paper is to investigate the response of all-polypropylene composites to mechanical loading at a range of temperatures and strain rates. By characterising these responses, mastercurves can be created in order to help predict the performance of all-PP composites at strain rates outside those achievable in the laboratory.

2. All-polypropylene composite manufacture

The all-PP composites described in this paper are composed of highly oriented PP tapes that have been woven into a plain weave fabric and consolidated into laminates. The entire composite fabrication process is described in full detail elsewhere [3,28,29], but is summarised here. PP tapes are co-extruded using two single screw extruders to produce a tape with a skin–core–skin (A:B:A) morphology, with a thickness ratio of 5.5:89:5.5. The core layer is a homopolymer blend composed of a 50:50 blend of two PP homopolymers with molecular weights (Mw) of 280 and 350 kg mol^{-1}, respectively, and a melting temperature of ~160 °C. The skin layer is a propylene:ethylene copolymer (Mw = 320 kg mol^{-1}) with a first melting peak endotherm of ~107 °C [4].

It is well known that polymers can be oriented to achieve molecular orientation and hence dramatically improved tensile properties in the direction of orientation, via a variety of routes [30]. To achieve a high degree of molecular alignment in these PP tapes and so attain the high mechanical properties required for the creation of competitive composites, this co-extruded tape is drawn in a continuous two-stage drawing process through a hot air oven. A draw ratio, λ, of 17 is achieved with approximate final tape dimensions of 2.15 mm width and 60 μm thickness, although lower draw ratio tapes were also produced, for research purposes [31]. During drawing, the tape is drawn to $\lambda = 17$, and has a tensile modulus of 15 GPa and a tensile strength of 450 MPa (see Table 1), which is almost entirely due to the highly oriented core layer of the tape that comprises the bulk of the tape [1]. Since the copolymer skin layer has a melting temperature below that of the highly oriented homopolymer core, these tapes can be effectively welded together by bonding them at temperatures which allow the interdiffusion of the isotropic copolymer skin layer without the molecular relaxation of the oriented homopolymer core layer [4]. Thus, these highly oriented PP tapes possess the potential to be bonded together without a loss in mechanical properties and all-PP composites can be created, although the composites described in this paper are produced by consolidating fabrics woven from these tapes.

After drawing, the tape is woven into a plain weave fabric with an areal density of ~100 g m^{-2}. This woven tape fabric is the precursor for composite laminate fabrication. Fabric plies are stacked in a close fitting mould with dimensions of 180 mm × 180 mm and heated to the compaction temperature under a pressure of 4 MPa. The all-PP composite laminates described in this paper are compacted at 140 °C. All-PP composites have previously been created with compaction temperatures ranging between 125 °C and 160 °C, and the effect of this compaction temperature on the mechanical properties of the resulting composite has been fully described elsewhere [3]. A compaction pressure is essential to prevent relaxation of the highly oriented structure and so prevent the loss of the mechanical properties of the woven tapes [32–35] and aid the consolidation of the fabric plies in a coherent composite laminate [3]. The resultant all-PP composite laminates created for this research have a thickness of ~1 mm and can be cut into testing specimens, with dimensions appropriate to the particular test. It must be emphasised that no additional material (reinforcement or matrix) is introduced during

Table 1
Summary of PP tape properties

Width	2.15 mm
Thickness	60 μm
Density, ρ	0.732 g cm^{-3}
Draw ratio, λ	17
Composition (copolymer:homopolymer:copolymer)	5.5:89:5.5
Tensile modulus	15 GPa
Tensile strength	450 MPa
Strain to failure	7%

composite consolidation; the entire composite is manufactured by bonding together co-extruded tape fabrics.

3. Experimental procedure

3.1. DMTA of single tapes

Dynamic mechanical thermal analyses (DMTA) were performed on co-extruded PP tapes, with draw ratios of $\lambda = 1$(undrawn), 4, 6, 12 and 17. Specimens were tested in a TA Instruments DMAQ800 DMTA machine operating in a tensile testing mode. A gauge length of 10 mm was used, and since all tapes were drawn from the same original co-extruded tape, thickness and width of tape decrease with increasing draw ratio. The test specimen was cooled to below −50 °C, allowed to stabilise and then heated at a rate of 1 °C min^{-1} to 160 °C. A static stress of 0.1 MPa was applied to ensure that the tape was taut between the tensile grips, and a sinusoidal (dynamic) tensile load was applied, to produce a dynamic strain with a constant maximum. The static stress was constant during testing to allow longitudinal shrinkage of the tape during heating.

3.2. DMTA of woven tape composites

DMTA of all-PP composites was performed in a dual cantilever flexure mode on woven tape composite plates manufactured as described earlier. Specimens were cut from these plates with dimensions of approximately 30 mm × 8 mm × 1 mm, either [0°/90°] to the tape direction or [±45°] to the tape direction. These specimens were tested in a Rheometric Scientific Mk II DMTA machine fitted with a dual cantilever bending test assembly and data acquisition software. The specimens were placed in the test grips inside a heating chamber and then the specimen and grips were cooled to below −80 °C, by the manual addition of liquid nitrogen to the chamber. The temperature was allowed to stabilise, and then the chamber was heated at a rate of 1 °C min^{-1} to 170 °C, although useful data above 165 °C was not achieved due to relaxation and shrinkage of the test specimen. The specimen was subjected to a sinusoidal flexural displacement applying a maximum tensile strain of 0.2% at frequencies of 100 Hz, 10 Hz, 1 Hz and 0.1 Hz. For each frequency, the dynamic modulus and the loss factor were recorded. The data acquisition at this heating rate provided data points at a rate of approximately 1 measurement per frequency per 2 min interval.

3.3. Estimation of heat distortion temperature (HDT)

The heat distortion temperature (HDT) test is a popular industry standard with little actual scientific value, used as a simple comparison of the thermal flexural stability of materials. The test is described fully in ASTM D648. The HDT test yields a single temperature value at which a mid-span deflection of 0.25 mm is attained, due to a static flexural load applied to the test specimen during exposure to increasing temperature at rate of 2 °C min^{-1}. The two standard loads used are 0.45 MPa and 1.82 MPa; only 1.82 MPa is considered in this research. Since this test specifies a flexural deformation and specimen dimensions, a flexural strain is also specified:

$$r = \frac{6dD}{L^2} \tag{1}$$

where r is the strain of outermost fibres; D, the midspan deflection; d, the specimen thickness and L is the span length. For the HDT test in ASTM D648, $d = 0.25$ mm, $D = 13$ mm, and $L = 100$ mm, giving $r = 0.195\%$. Therefore, the HDT test can be interpreted to specify the temperature at which a certain strain is achieved. Moreover, since the applied stress of 1.82 MPa is constant, the HDT temperature can be considered to specify the temperature at which a flexural modulus of 0.93 GPa is achieved. The standard HDT test involves the static loading of a body. Thus molecular relaxation processes may operate, but if these are ignored, the HDT test can be compared to DMTA of plates, as described above, since DMTA also describes the relationship between modulus and temperature.

3.4. Static tensile testing at elevated temperatures

Static tensile tests were performed on woven tape composite plates at a range of discrete temperatures between −40 °C and 150 °C using an Instron 5584 tensile testing machine, equipped with a 5 kN load cell and data acquisition software. Specimens were placed in composite grips which allow 10° free rotation to reduce the effect of moments in the off-axis specimens. To achieve the desired range of testing temperatures, an Instron 3119 environmental chamber was fitted to the tensile testing machine. This chamber is a circulating air oven and with a liquid nitrogen supply to control temperature and allow sub-ambient temperatures to be reached. A gauge length of 70 mm and a crosshead displacement speed of 5 mm min^{-1} were used, giving an initial strain rate of 1.2×10^{-3} s^{-1}. The specimens were fitted between tensile testing grips at room temperature and then the chamber was cooled/heated to testing temperature. The temperature was held for 5 min to allow uniform temperature within the specimen, and then tensile testing was commenced. The tensile moduli were determined using a thermally stable Instron clip-on extensometer and the moduli were measured in a strain range of 0.05–0.2%, which proved to be a linear and reproducible region in all cases. For each temperature, a minimum of 5 repetitions were performed.

3.5. Time–temperature superposition of polymers

Experimental data determining the dynamic response of a polymer loaded at different strain rates is limited by the range of strain rates which can practically be applied for a particular test method. It is desirable to obtain informa-

tion about strain rates outside the range that can be achieved experimentally, in order to predict the behaviour of materials over very long loading times. By assuming equivalence of time and temperature, the viscoelastic behaviour of a polymer at a chosen reference temperature, T_{ref}, can be related to the viscoelastic behaviour of the polymer at a different temperature by a shift, a_T, in the time-scale [36].

Practically, data is obtained at the widest range of strain rates experimentally possible, at a range of temperatures. This data can then be shifted by a_T to higher or lower time scales since these are equivalent at higher or lower temperatures; lower temperature experimental data provides information about shorter loading rates and vice versa. This shift factor can be modelled using an Arrhenius equation [37,38]. The result of shifting data in this way is a mastercurve of data which provides a much wider range of information than experimentally possible for the reference temperature, T_{ref}. It is also widely accepted that a minor vertical shift factor may also be applied to more accurately model mastercurves [36]. However, in this study, a vertical shift was not applied since this was only seen to make a significant effect at extremes of strain rate, where the prediction of mechanical properties is inherently much less accurate.

In order to use mastercurves to predict the long term behaviour of polymers, the polymer must show a constant temperature dependence and a constant thermal activation energy, E_a. While the prediction of mechanical behaviour of amorphous polymers is possible, these mastercurve predictions grossly oversimplify the complex behaviour seen in semi-crystalline polymers which may possess numerous thermal transitions and an irregular temperature dependence.

In the case of a thermo-rheologically simple material, the shift factor, a_T, can be given by Eq. (2)

$$\ln a_T = \frac{E_a}{R}\left(\frac{1}{T} - \frac{1}{T_{ref}}\right) \tag{2}$$

where a_T is the shift factor; E_a, the activation energy for the change in property; R, the universal gas constant [8.314 J mol^{-1} K^{-1}]; T, the absolute temperature of data to be shifted and T_{ref} is the absolute reference temperature of data. Using this shift factor, a_T, it is possible to create a mastercurve to predict the mechanical behaviour over a much wider range of strain rates at a single reference temperature, T_{ref}. The use of these techniques assumes time and temperature equivalence and does not include any allowance for degradation or aging of the polymer due to environmental effects, which may occur due to actual loading at large time scales.

3.6. Reference materials

In addition to co-extruded PP tapes and all-PP composites presented in this paper, two popular types of commercial glass reinforced polypropylenes are reported for comparison. The first is Symalite® [57] (hereafter referred to as GMT), and is a random, discontinuous glass reinforced PP with a fibre weight fraction of 23% and was supplied in 4 mm thick sheets. The second, Twintex® [56], is a balanced, woven glass reinforced PP with a fibre weight fraction of 40% and supplied in 2.3 mm thick sheets.

4. Results and discussion

4.1. Dynamic thermal mechanical behaviour of individual tapes

The effect of temperature on the dynamic modulus, E^*, of a range of tapes with increasing draw ratio at a frequency of 1 Hz is shown in Fig. 1. Also shown for comparison in Fig. 1 is the dynamic modulus of an undrawn PP tape. The dynamic moduli of these tapes clearly decreases with increasing temperature as would be expected. Each of the tapes show a curve that is similarly shaped to the undrawn (isotropic) specimen and in the case of drawn tapes, the dynamic modulus increases with increasing draw ratio.

Fig. 2 shows this data as a function of draw ratio. Dynamic modulus at room temperature increases almost linearly with draw ratio. At −50 °C, the dynamic modulus for each draw ratio is 4 GPa ± 0.8 greater than the dynamic modulus at 20 °C. At 120 °C, lower draw ratio tapes ($\lambda = 4$ and 6), possess similar dynamic moduli (<0.5 GPa) as undrawn PP. This suggests that these lower draw ratio tapes have totally relaxed at 120 °C and reflects the lower thermal stability of these low draw ratio tapes as seen in early results predating this paper [29].

The higher draw ratio tapes, $\lambda = 12$ and 17, retain a higher modulus at elevated temperatures, possessing dynamic moduli of 1.5 GPa and 3.7 GPa, respectively, at 120 °C. These values are similar to those reported for PP oriented to similar draw ratios by roll drawing [39,40]

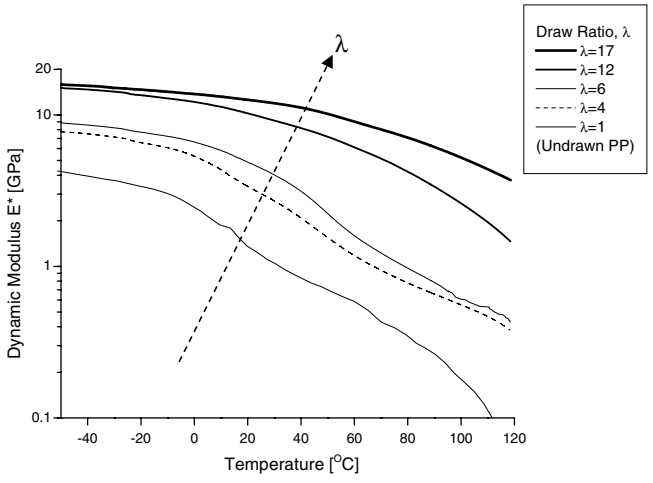

Fig. 1. Dynamic modulus vs. temperature for a range of PP tapes with increasing draw ratio showing the greater temperature stability of more highly oriented PP tapes (note: log scale of y-axis).

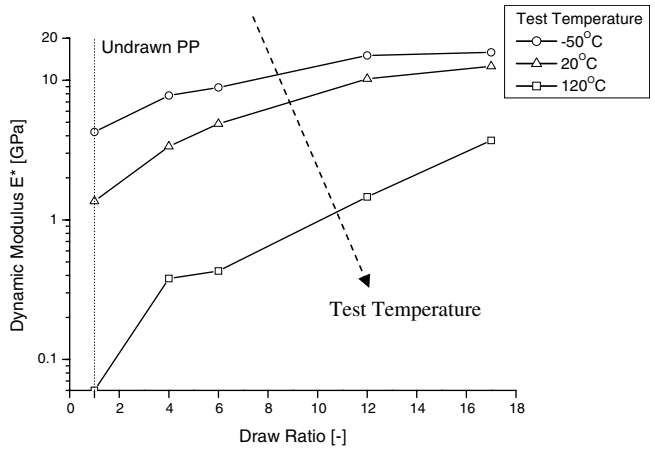

Fig. 2. Dynamic modulus vs. draw ratio for a range of PP tapes with increasing test temperature showing highly drawn PP tapes possess greater dynamic modulus at 120 °C than undrawn PP possesses at 20 °C, and so some degree of orientation is still present at this temperature (note: log scale of *y*-axis).

and hot air drawing [41]. This data shows that a tape drawn to $\lambda = 17$ still possesses a greater dynamic modulus at 120 °C than undrawn PP possesses at 20 °C, so there is still residual orientation even at these high temperatures.

Fig. 3 shows the variation of loss factor, $\tan\delta$, with temperature for tapes with draw ratios $\lambda = 1$(undrawn), 4, 6, 12 and 17. Firstly a decrease in sub-T_g tan δ is seen with increasing λ. This can be explained by the increasing orientation (and so order) of interlamellar amorphous PP, with increasing draw ratio [42]. A similar trend in loss factor was also reported for LDPE oriented by hydrostatic extrusion [43], with the loss factor decreasing with increasing draw ratio, λ.

In Fig. 3, the undrawn (isotropic) specimen shows a peak in tan δ at approximately 0 °C. This is associated with the glass transition temperature, T_g, (β relaxation) of isotactic PP [39,44], although it is not possible to exactly define the value of T_g from this graph since the peak is rather broad. A similar peak is seen in the tape drawn to $\lambda = 4$, although the peak is shifted to a slightly higher temperature, and the height of the peak is reduced. There is a suggestion of a peak in $\tan\delta$ for the tape drawn to $\lambda = 6$, but much reduced in magnitude. Since this $\tan\delta$ peak is associated with T_g, it is reasonable to expect a reduced effect of T_g for tapes with higher draw ratio, as with increasing draw ratio the amorphous phase of PP becomes oriented along the drawing direction [45]. If the amorphous phase becomes highly oriented between crystalline regions and forms taut tie molecules, it has less freedom to engage in small segmental motions [40,46]. Therefore, in highly oriented PP systems, the magnitude of glass transition peaks normally seen in isotropic PP are greatly reduced. This can also be seen in Fig. 1, in which no significant decrease in dynamic modulus of highly oriented PP ($\lambda = 17$) is seen around the normal glass transition temperature. The highly oriented amorphous phase can be given sufficient energy to allow these conformational changes to occur, but requires greater thermal energy than in unoriented PP. This is reflected in the slight increase of T_g with increasing λ shown in Fig. 3. From Fig. 1, the most noticeable decrease in the dynamic modulus of the tape drawn to $\lambda = 17$ occurs at 50 °C, and this could account for a glass transition effect which has been shifted to higher temperatures by the high degree of orientation of the amorphous phase.

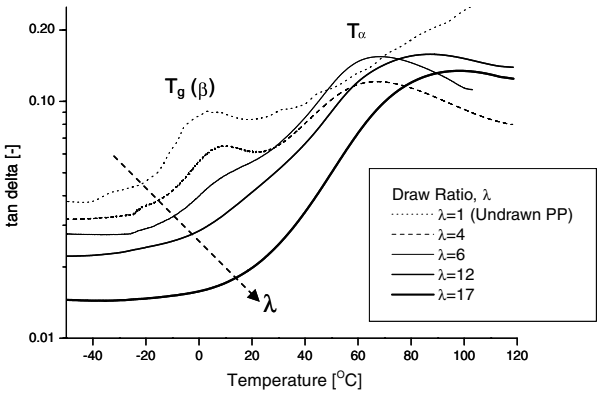

Fig. 3. Loss factor vs. draw ratio for a range of PP tapes with increasing test temperature. This graph shows a gradually decrease in the magnitude of T_g and a shift to higher T_g with increasing draw ratio (note: log scale of *y*-axis).

Fig. 3 shows another peak in $\tan\delta$ occurring at higher temperatures than associated with T_g. The temperature of this α transition, T_α, increases with increasing draw ratio. While T_g concerns mobility within the amorphous regions, T_α dictates the onset of segmental motion within the crystalline regions (chain diffusion) [46–48]. As draw ratio increases from $\lambda = 4$ to 6, the magnitude of the T_α peak in $\tan\delta$ becomes larger. The greater crystal continuity, and greater crystalline stem length, achieved by high draw ratios seems to result in a higher temperature requirement for this T_α transition to occur. As λ reaches 12 and 17, the tapes become more thermally stable due to the drawn structure, and the greater crystalline stem length requires greater thermal energy to allow conformational changes [49].

4.2. Dynamic thermal mechanical behaviour of woven tape composites

All of the all-PP composites were manufactured from woven tape with a draw ratio $\lambda = 17$ and were tested in a dual cantilever bending mode either [0°/90°] or [±45°] to the tape direction. These composites show a similar dynamic response to the individual tape ($\lambda = 17$) presented earlier. Fig. 4 shows the dynamic modulus of an all-PP composite plate compared to a plate of isotropic PP.

All-PP specimens show the same behaviour when tested at [0°/90°] or [±45°] to the tape direction (see Fig. 4). Since

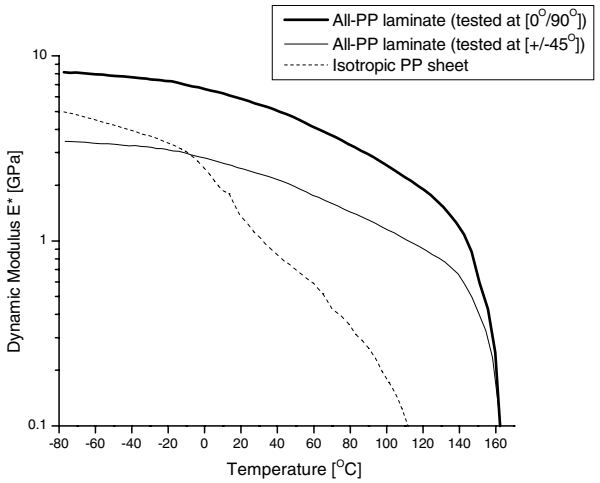

Fig. 4. Dynamic modulus vs. temperature for all-PP composites tested at 0°/90° and ±45° to tape direction. Compared to an isotropic PP sheet, the all-PP composites do not show a significant glass transition (note: log scale of *y*-axis).

loading in the [±45°] direction does not transfer forces along the tape direction, the dynamic modulus is lower than for [0°/90°] specimens. The proportional difference between composites tested at [0°/90°] to tape direction and [±45°] to tape direction is approximately 45% and is the same as the difference seen in static tensile testing of these composites [3]. The loss factor as a function of temperature for all-PP composites compared to isotropic PP, is shown in Fig. 5. The trend is the same as seen in Fig. 3 (note that the tapes present in all of the all-PP composites described here are drawn to $\lambda = 17$). As in the DMTA data from the single tape, composite specimens do not show a clear peak in $\tan\delta$ (attributable to glass transition) in Fig. 5. A more definite peak is seen in $\tan\delta$ corresponding to T_α at approximately 90 °C.

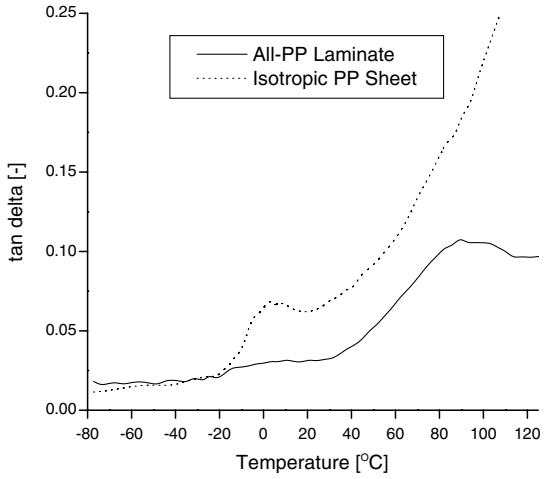

Fig. 5. Tan delta loss factor vs. temperature for an all-PP composite laminate compared to an isotropic PP sheet. Unlike the isotropic PP sheet, the all-PP composite does not show a significant glass transition, and this is reflected in a negligible decrease in dynamic moduli near T_g as seen in Fig. 4.

Having established the effect of temperature on the dynamic modulus of all-PP composites, a heat distortion temperature can be estimated, as described in Section 3.3. The dynamic modulus value, which approximates the HDT at a stress of 1.82 MPa, is shown in Fig. 6. The values estimated by DMTA for GMT compare very well with those reported by conventional HDT testing in literature [50]. The HDT values are presented in Table 2, which compares this method with manufacturers data obtained using standard HDT test equipment, and shows that HDT approximations by DMTA provide a good correlation in each case. It must be emphasised that determining HDT by DMTA is an estimation and does not account for thermal relaxation of the specimen which may occur in static HDT testing but not in the DMTA comparison. This means that DMTA should overestimate the HDT, due to the absence of creep in the dynamic method. However, the HDT values estimated for both the GMT and woven glass reinforced PP represent a flexural deformation near the melting point of PP so a total collapse of the specimen would be expected at these temperatures. It is clear that the HDT of all-PP composites is 100 °C greatly than isotropic PP and only 20 °C less than GMT.

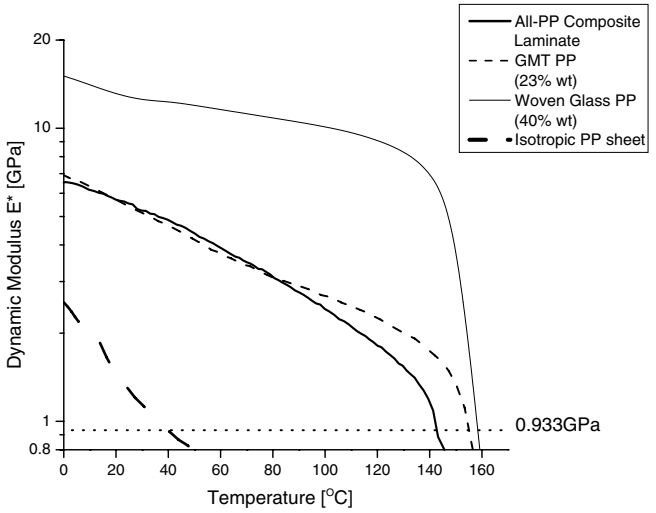

Fig. 6. Dynamic modulus vs. temperature for an all-PP composite, isotropic PP, woven glass PP and GMT (all-PP and woven glass PP tested at 0°/90° to tape/fibre direction). The modulus of 0.933GPa is associated with the flexural modulus experienced in static heat distortion tests.

Table 2
Table of heat distortion temperatures estimated from DMTA compared heat distortion temperature results from literature

Material	HDT estimation (DMTA) [°C]	HDT (ASTM D648) [°C]
Woven glass PP (40 wt.%)	158.6	159 [56]
GMT (23 wt.%)	154	155 [57]
All-PP composite	134	–
Undrawn PP	36	–

4.3. Static mechanical properties of woven tape composites at elevated temperatures

To further clarify the static properties of all-PP composites at elevated temperatures, tensile tests were performed on woven tape all-PP composite tensile specimens at a range of discrete temperatures. The modulus of all-PP composites loaded along the [0°/90°] tape direction at a range of temperatures is shown in Fig. 7, and compared to GMT. The comparison with GMT is important since the reinforcing component of GMT, i.e. glass fibres, is not greatly affected by temperature in the temperature range investigated here.

These results show similar trends to those obtained by DMTA. The static tensile modulus of the all-PP composite is higher than GMT at temperatures below 40 °C and lower above 40 °C. This is unlike the DMTA results, in which the two materials have similar dynamic moduli between 20 °C and 80 °C (see Fig. 6); outside this region, GMT has a higher dynamic modulus than the all-PP composite. The approximately linear behaviour of the tensile modulus of GMT with increasing temperature (between 20 °C and 120 °C) has previously been reported [50], although a decrease in dynamic modulus at T_g is also reported but this decrease is not clearly visible in Fig. 7.

The strength of these composites at elevated temperatures also provides useful comparative data on the possible application temperature of all-PP composites. This information is shown in Fig. 8. With increasing testing temperature, the tensile strength of both the all-PP and the GMT specimens decreases; the decrease in strength of the all-PP composite can be seen to decrease in two approximately linear regions, with a transition at approximately 90 °C, which coincides with T_α shown in Fig. 5. Since α transitions are associated with increased molecular mobility within the crystalline phase, this rapid decrease in strength above T_α may be due to the reduced shear strength of the crystals at this temperature [51].

The work absorbed in tensile failure has been measured from all-PP composite specimens and is presented in Fig. 9.

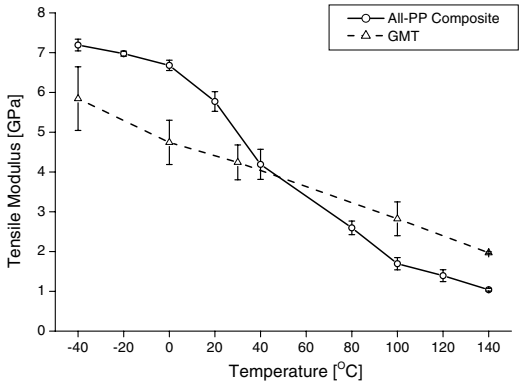

Fig. 7. The tensile modulus of all-PP composites and GMT vs. temperature. The tensile modulus of the all-PP composite is greater than GMT at temperatures below 40 °C.

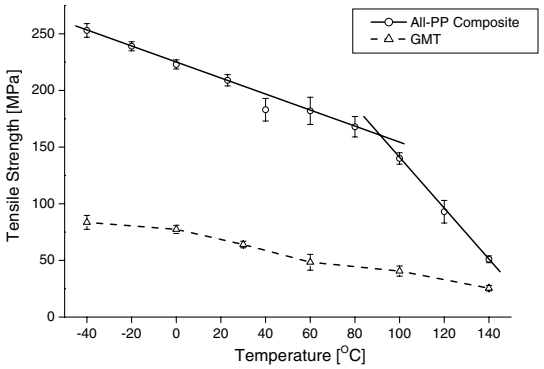

Fig. 8. The tensile strength of all-PP composites and GMT vs. temperature showing that the tensile strength of all-PP decreases with increasing temperature in two linear regions, with a transition at ~90 °C.

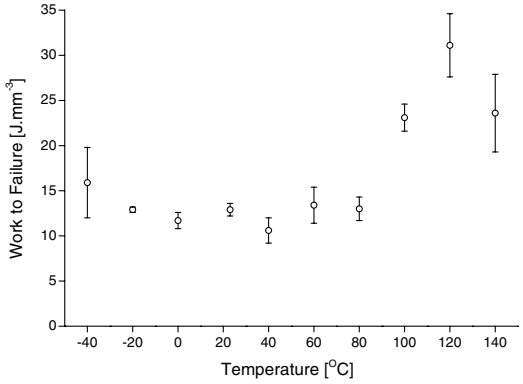

Fig. 9. The work absorbed in failure of all-PP composites when tested in tension at a range of discrete temperatures. An increase in work absorbed in failure is seen as testing temperature exceeds 90 °C reflecting an increase in ductility.

The work to failure during tensile failure is approximately constant up to approximately 90 °C, since the same failure modes of tape breakage and delamination operate. As T_α is reached (see Fig. 5), there is a sudden increase in toughness due to greater strain to failure of the composite. This may be attributed to increased mobility within the crystals allowing the tape to yield more easily in tension, so encouraging greater deformation before failure. This suggests that while the modulus is governed by a contribution of highly oriented amorphous phase together with the crystalline phase, the tensile strength is mainly governed by the crystalline phase. This may explain why no effect of T_g is seen on the tensile strength of the all-PP composites, since T_g affects the amorphous regions, but an effect due to T_α on the crystalline phase is clearly visible.

4.4. Time–temperature superposition of dynamic modulus and static strength data of woven tape composites

Using the principle of time–temperature superposition (described in Section 3.5), data obtained from DMTA and static tensile tests can be adapted to predict the dynamic modulus at a wider range of frequencies. Fig. 10

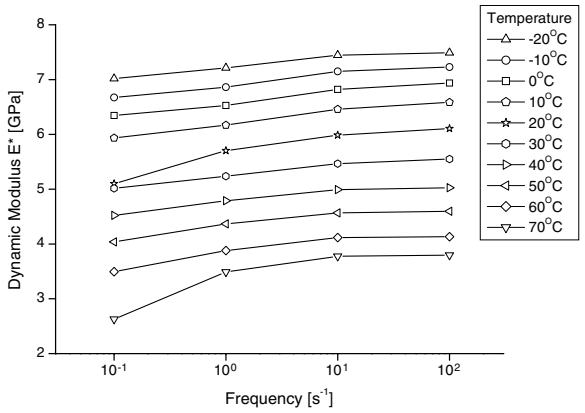

Fig. 10. Dynamic modulus vs. frequency for a range of temperatures, showing an increase of dynamic modulus with increasing frequency and decreasing temperature.

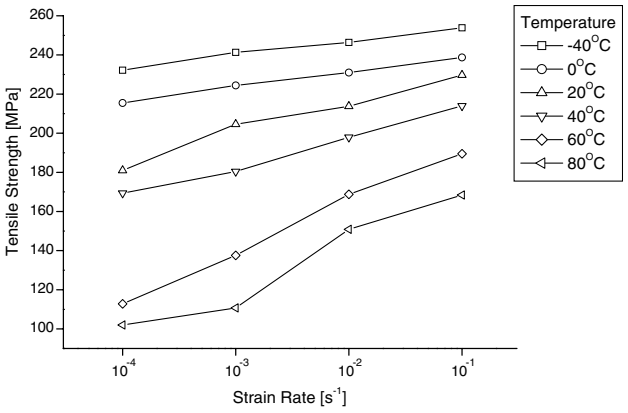

Fig. 12. Tensile strength vs. strain rate for a range of temperatures showing an increase in tensile strength with increasing strain rate and decreasing temperature.

shows the variation of dynamic modulus for a range of temperature between −20 °C and 70 °C, tested in DMTA at strain rates of 100 Hz, 10 Hz, 1 Hz and 0.1 Hz. Using a horizontal shift factor a_T, these can be shifted to create a mastercurve at a reference temperature of 20 °C. Fig. 11 shows the dynamic modulus mastercurve created by horizontal shifting of these data.

A similar process can be used to create a mastercurve of tensile strength. Tensile tests are performed in a tensile test machine (see Section 3.4), but at a three decade range of strain rates. These results can be combined to provide a tensile strength mastercurve, expanding the strain rate range. In this case, a different shift factor is required. Fig. 12 shows the tensile strength of the all-PP composite as a function of strain rate at a range of temperatures. By applying a horizontal shift factor, a strength mastercurve can be created and this is shown in Fig. 13. The shift factors used in Figs. 11 and 13 are shown in Fig. 14. The activation energy E_a can be determined from Eq. (3)

$$E_a = m(2.303R) \tag{3}$$

where m is the gradient of fit line in Fig. 14 and R is the universal gas constant. Both shift factors show approximately constant values (as indicated by the r^2 fit parameter) with an activation energy of ~300 kJ mol^{-1} and ~100 kJ mol^{-1} for dynamic flexural modulus and static tensile strength, respectively. Since, when the curves are shifted to create the mastercurves, an approximately constant a_T is found, the extrapolation appears to be valid.

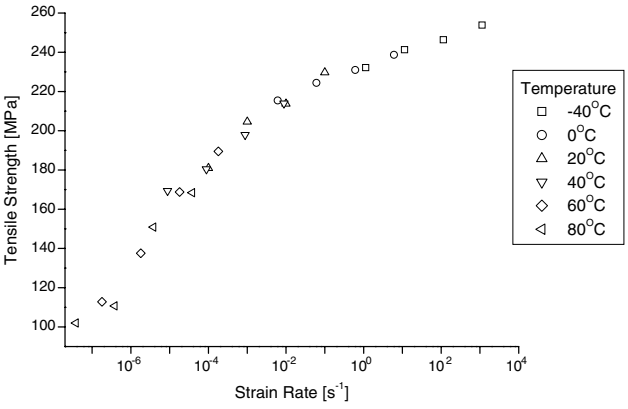

Fig. 13. Strength mastercurve for a reference temperature of 20 °C created from data shown in Fig. 12.

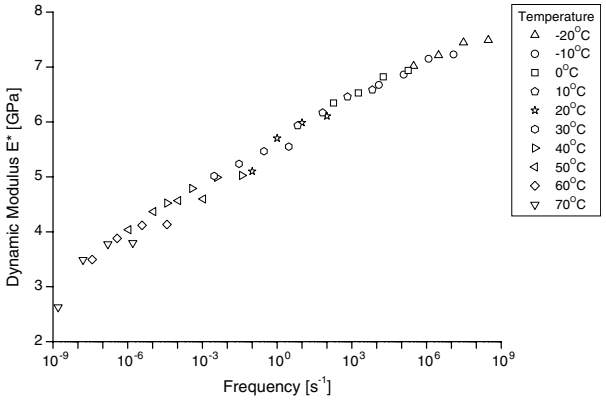

Fig. 11. Dynamic modulus mastercurve for a reference temperature of 20 °C created from data shown in Fig. 10.

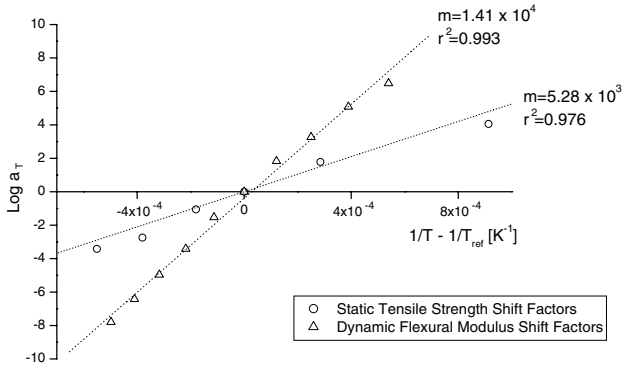

Fig. 14. Determination of activation energy for time–temperature superposition of static tensile strength and dynamic flexural modulus.

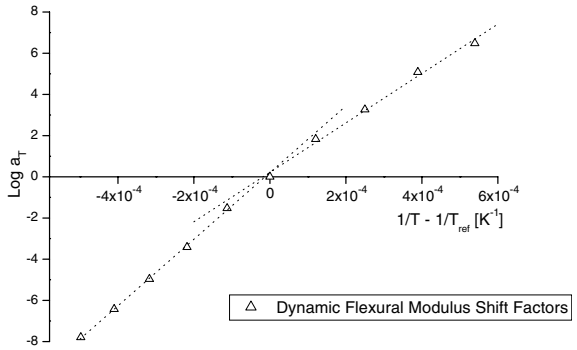

Fig. 15. Non-uniform activation energy for time–temperature superposition of dynamic modulus.

An activation energy of 300 kJ mol^{-1} is used to shift the dynamic modulus mastercurve, which is of the same order as previously reported using the same simple Arrhenius shifting of PP: 210 kJ mol^{-1} [37,52], 273 kJ mol^{-1} [53] and 364 kJ mol^{-1} [54]. Although Arrhenius shifting has been shown to be empirically successful, the validity of time–temperature superposition of PP as a thermo-rheologically simple material has been queried and it has been previously reported that using a simple Arrhenius shift can yield unrealistically high activation energies [55]. Since a single activation energy leads to a good fit of the modulus data it is likely that the same mechanisms are occurring across the strain rate range, which is likely since the temperature range here is relatively small. It is likely that this 'activation energy' describes a complex combination of effects since simple time–temperature superposition is only directly applicable to amorphous polymers. The mastercurve provides a useful prediction of the modulus over loading times from 10^{-9} to 10^{9} s, i.e. from nanoseconds to multiple year time scales. However, it must be stressed that these mastercurves provide a *prediction* of behaviour that may be quite valid over relatively short time scales i.e. $<10^{6}$ s, but significant deviations are to be expected at greater time scales.

On closer analysis of Fig. 14, it can be interpreted that the data points for the dynamic flexural modulus shift factors are better fitted by two lines, as shown in Fig. 15. This suggests a non-uniform temperature dependent activation energy and thus reduces confidence in the validity of the time–temperature superposition principle, when applied to highly oriented PP. However, since these trend lines are still of a very similar gradient, it is likely that the effect is negligible over this relatively small range of temperature described here. This further illustrates the complexity of modelling the PP as a thermo-rheologically simple polymer.

5. Conclusion

All-PP composites have been created which possess similar mechanical properties to traditional glass fibre reinforced PPs. As a result of the high degree of molecular orientation present in the all-PP precursor tapes, a significant glass transition is not seen in dynamic mechanical testing. This is advantageous as it results in a tough failure mode at sub-zero (sub-T_g) temperatures and hence has positive implications for application of all-PP composites at low temperatures or high strain rates.

The effect of temperature and strain rate on the mechanical properties of all-PP composites has been analysed and tensile modulus and strength data has been used to create strength and modulus mastercurves, by assuming time–temperature superposition with an Arrhenius fit of data. These mastercurves can be used to predict the response of all-PP composites to extremes of temperature or strain rate not easily achievable in the laboratory.

Acknowledgements

The authors would like to acknowledge the contribution of Dr. Edwin Klompen at Eindhoven University of Technology, Netherlands, to this project. The co-extruded PP tapes used in this study were kindly supplied by Lankhorst Indutech BV, Netherlands. This work is sponsored by the Dutch Government's Economy, Ecology and Technology (EET) programme for sustainable development, under Grant Number EETK97104.

References

[1] Alcock B, Cabrera NO, Barkoula N-M, Loos J, Peijs T. The mechanical properties of unidirectional all-polypropylene composites. Composites: Part A 2006;37(5):716–26.
[2] Alcock B, Cabrera NO, Barkoula N-M, Peijs T. Low velocity impact performance of recyclable all-polypropylene composites. Compos Sci Technol 2006;66(11–12):1724–37.
[3] Alcock B, Cabrera NO, Barkoula N-M, Spoelstra AB, Loos J, Peijs T. The mechanical properties of woven tape all-polypropylene composites. Composites: Part A 2007;38(1):147–61.
[4] Alcock B, Cabrera NO, Barkoula N-M, Loos J, Peijs T. Interfacial properties of highly oriented co-extruded polypropylene tapes for the creation of recyclable all-polypropylene composites. J Appl Polym Sci, in press.
[5] Abo El-Maaty MI, Bassett DC, Olley RH, Hine PJ, Ward IM. The hot compaction of polypropylene fibres. J Mater Sci 1996;31:1157–63.
[6] Hine PJ, Ward IM, Teckoe J. The hot compaction of woven polypropylene tapes. J Mater Sci 1998;33:2725–33.
[7] Jordan ND, Bassett DC, Olley RH, Hine PJ, Ward IM. The hot compaction behaviour of woven oriented polypropylene fibres and tapes. II. Morphology of cloths before and after compaction. Polymer 2003;44:1133–43.
[8] Hine PJ, Ward IM, Jordan ND, Olley RH, Bassett DC. The hot compaction behaviour of woven oriented polypropylene fibres and tapes. I. Mechanical properties. Polymer 2003;44:1117–31.
[9] Hine PJ, Ward IM, Olley RH, Bassett DC. The hot compaction of high modulus melt-spun polyethylene fibres. J Mater Sci 1993;28:316–24.
[10] Yan PJ, Hine PJ, Ward IM, Olley RH, Bassett DC. The hot compaction of spectra gel-spun polyethylene fibre. J Mater Sci 1997;32:4821–31.
[11] Megremis SJ, Duray S, Gilbert JL. Self reinforced composite polyethylene (SRC-PE): a novel material for orthopaedic applications. ASTM Spec Tech Publ 1999;1346:235–55.
[12] Hine PJ, Ward IM, Jordan ND, Olley RH, Bassett DC. A comparison of the hot-compaction behavior of oriented, high-

modulus, polyethylene fibers and tapes. J Macromol Sci: Phys 2001;B40(5):959–89.
[13] Jordan ND, Olley RH, Bassett DC, Hine PJ, Ward IM. The development of morphology during hot compaction of tensylon high-modulus polyethylene tapes and woven cloths. Polymer 2002;43:3397–404.
[14] Xu T, Farris RJ. Shapeable matrix-free spectra((*R*)) fiber-reinforced polymeric composites via high-temperature high-pressure sintering: process–structure–property relationship. J Polym Sci Part B – Polym Phys 2005;43(19):2767–89.
[15] Rasburn J, Hine PJ, Ward IM, Olley RH, Bassett DC, Kabeel MA. The hot compaction of polyethylene terephthalate. J Mater Sci 1995;30:615–22.
[16] Hine PJ, Ward IM. Hot compaction of woven poly(ethylene terephthalate) multifilaments. J Appl Polym Sci 2004;91(4):2223–33.
[17] Rojanapitayakorn P, Mather PT, Goldberg AJ, Weiss RA. Optically transparent self-reinforced poly(ethylene terephthalate) composites: molecular orientation and mechanical properties. Polymer 2005;46(3):761–73.
[18] Hine PJ, Astruc A, Ward IM. Hot compaction of polyethylene naphthalate. J Appl Polym Sci 2004;93(2):796–802.
[19] Gilbert JL, Ney DS, Lautenschlager EP. Self-reinforced composite poly(methyl methacrylate) – static and fatigue properties. Biomaterials 1995;16(14):1043–55.
[20] Wright DD, Lautenschlager EP, Gilbert JL. Bending and fracture toughness of woven self-reinforced composite poly(methyl methacrylate). J Biomed Mater Res 1996;36:441–53.
[21] Wright DD, Gilbert JL, Lautenschlager EP. The effect of processing temperature and time on the structure and fracture characteristics of self-reinforced composite poly(methyl methacrylate). J Mater Sci: Mater Med 1999;10:503–12.
[22] Wright-Charlesworth DD, Lautenschlager EP, Gilbert JL. Hot compaction of poly(methyl methacrylate) composites based on fiber shrinkage results. J Mater Sci – Mater Med 2005;16(10):967–75.
[23] Hine PJ, Ward IM. Hot compaction of woven nylon 6,6 multifilaments. J Appl Polym Sci 2006;101(2):991–7.
[24] Pegoretti A, Zanolli A, Migliaresi C. Flexural and interlaminar mechanical properties of unidirectional liquid crystalline single-polymer composites. Compos Sci Technol 2006;66(13):1953–62.
[25] Pegoretti A, Zanolli A, Migliaresi C. Preparation and tensile mechanical properties of unidirectional liquid crystalline single-polymer composites. Compos Sci Technol 2006;6(13):1970–9.
[26] Rokkanen PU, Bostman O, Hirvensalo E, Makela EA, Partio EK, Patiala H, et al. Bioabsorbable fixation in orthopaedic surgery and traumatology. Biomaterials 2000;21(24):2607–13.
[27] Wright-Charlesworth DD, Miller DM, Miskioglu I, King JA. Nanoindentation of injection molded PLA and self-reinforced composite PLA after in vitro conditioning for three months. J Biomed Mater Res Part A 2005;74A(3):388–96.
[28] Cabrera N. Recyclable all-polypropylene composites: concept, properties and manufacturing. Ph.D. thesis, Technische Universiteit Eindhoven, Netherlands, 2004.
[29] Alcock B. Single polymer composites based on polypropylene: processing and properties. Ph.D. thesis, Queen Mary, University of London, UK, 2004.
[30] Ward IM, editor. Structure and properties of oriented polymers. Kluwer Academic Publishers; 1997.
[31] Loos J, Schimanski T. Effect of postdrawing temperature on structure, morphology, and mechanical properties of melt-spun isotactic polypropylene tapes. Macromolecules 2005;38(26):10678–85.
[32] Lacroix F, Loos J, Schulte K. Morphological investigations of polyethylene fibre reinforced polyethylene. Polymer 1999;40:843–7.
[33] Bastiaansen CWM, Lemstra PJ. Melting behaviour of gel-spun/drawn polyolefins. Macromolecular Symposia 1989;28(28):73–84.
[34] Barkoula N-M, Schimanski T, Loos J, Peijs T. Processing of single polymer composites using the concept of constrained fibers. Polym Compos 2004;26(1):114–20.
[35] Loos J, Schimanski T, Hofman J, Peijs T, Lemstra PJ. Morphological investigation of polypropylene single-fibre reinforced polypropylene model composites. Polymer 2001;42:3827–34.
[36] Ward IM, Sweeney J. An introduction to the mechanical properties of solid polymers. John Wiley and Sons, Ltd.; 2004.
[37] Ariyama T, Mori Y, Kaneko K. Tensile properties and stress relaxation of polypropylene at elevated temperatures. Polym Eng Sci 1997;37(1):81–90.
[38] Djokovic V, Kostoski D, Dramicanin MD. Viscoelastic behaviour of semicrystalline polymers at elevated temperatures on the basis of a two-process model for stress relaxation. J Polym Sci: Part B: Polym Phys 2000;38:3239–46.
[39] Yang J, Chaffey CE, Vancso GJ. Structure, transitions, and mechanical properties of polypropylene oriented by roll-drawing. Plast Rubber Compos Process Appl 1994;21(4):201–10.
[40] Taraiya AK, Richardson A, Ward IM. Production and properties of highly oriented polypropylene by die drawing. J Appl Polym Sci 1987;33:2559–79.
[41] Unwin AP, Bower DI, Ward IM. Interpretation of the extensional modulus of oriented isotactic polypropylene using the aggregate and fibre composite models. Polymer 1990;31:882–9.
[42] Gibson AG, Davies GR, Ward IM. Dynamic mechanical behaviour and longitudinal crystal thickness measurements on ultra-high modulus linear polyethylene: a quantitative model for the elastic modulus. Polymer 1978;19:683–93.
[43] Gibson AG, Jawad SA, Davies GR, Ward IM. Shear and tensile relaxation behaviour in oriented linear polyethylene. Polymer 1982;23:349–58.
[44] Botev M, Neffati R, Rault J. Mobility and relaxation of amorphous chains in drawn polypropylene: 2H-NMR study. Polymer 1999;40(18):5227–32.
[45] Jawad SA, Alhaj-Mohammad MH. Beta-relaxation of drawn isotactic polypropylene in terms of a simplified two phase model. Polym Int 1994;35:395–8.
[46] Boyd RH. Relaxation processes in crystalline polymers: molecular interpretation – a review. Polymer 1985;26:1123–33.
[47] Hu WG, Schmidt-Rohr K. Polymer ultradrawability: the crucial role of alpha relaxation chain mobility in the crystallites. Acta Polym 1999;50:271–85.
[48] Seguela R, Staniek E, Escaig B, Fillon B. Plastic deformation of polypropylene in relation to crystalline structure. J Appl Polym Sci 1999;71:1873–85.
[49] Roy SK, Kyu T, St. John Manley R. Mechanical relaxations of oriented gelation-crystallized polyethylene films. Macromolecules 1988;21:1741–6.
[50] Schledjewski R, Karger-Kocsis J. Dynamic mechanical analysis of glass mat-reinforced polypropylene(GMT-PP). J Thermoplast Compos Mater 1994;7:270–7.
[51] Wills AJ, Capaccio G, Ward IM. Plastic deformation of polypropylene: effect of molecular weight on drawing behavior and structural characteristics of ultra-high modulus products. J Polym Sci: Polym Phys Ed 1980;18:493–509.
[52] Faucher JA. Viscoelastic behavior of polyethylene and polypropylene. Trans Soc Rheol (J Rheol) 1959;3:81–93.
[53] Klompen ETJ, Govaert LE. Nonlinear viscoelastic behaviour of thermorheologically complex materials. Mech Time-Dependent Mater 1999;3:46–69.
[54] Amash A, Zugenmaier P. Thermal and dynamic mechanical investigations on fiber-reinforced polypropylene composites. J Appl Polym Sci 1996;63:1143–54.
[55] Fytas G, Ngai KL. Study of viscoelastic relaxation in amorphous polypropylene near T_g by dynamic light scattering and shear creep. Macromolecules 1988;21:804–11.
[56] Saint Gobain-Vetrotex. 2003. Available at: www.twintex.com.
[57] Quadrant Plastic Composites. 2003. Available at: www.quadrantcomposites.com.